In silico comparison of rifampicin and 25-desacetyl rifampicin-induced PXR-mediated CYP450 transcriptional response in 3D primary human hepatocytes

Supplementary Information

Ellen Tanaka Kahiya[1], Tomáš Smutný[2], Lucie Smutná[2], Jurjen Duintjer Tebbens[1,3], Petr Pávek[2], and Veronika Bernhauerová[1✉]

[1]Department of Biophysics and Physical Chemistry, Faculty of Pharmacy, Charles University, Hradec Králové, Czech Republic

[2]Department of Pharmacology and Toxicology, Faculty of Pharmacy, Charles University, Hradec Králové, Czech Republic

[3]Department of Artificial Intelligence, Institute of Computer Science of the Czech Academy of Sciences, Prague, Czech Republic

[✉]Corresponding author: bernhauve@faf.cuni.cz

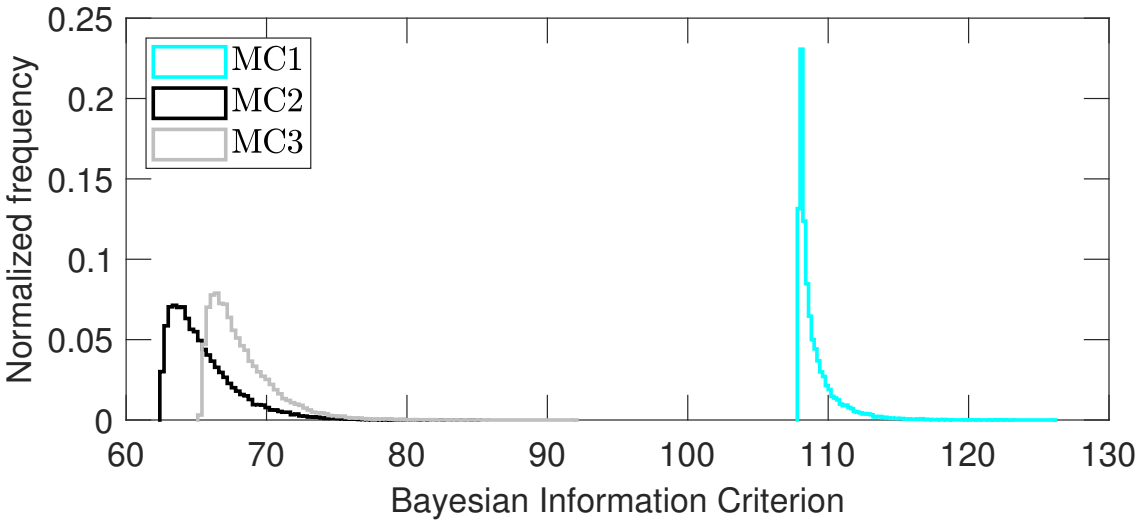

Figure S1: Bayesian Information Criterion (BIC). The BIC was constructed using the log-likelihood values obtained by fitting Equations (5)–(8) to the CYP mRNA fold expression data for the model configurations MC1 (cyan), MC2 (black), and MC3 (grey). Lower BIC values indicate better model performance.

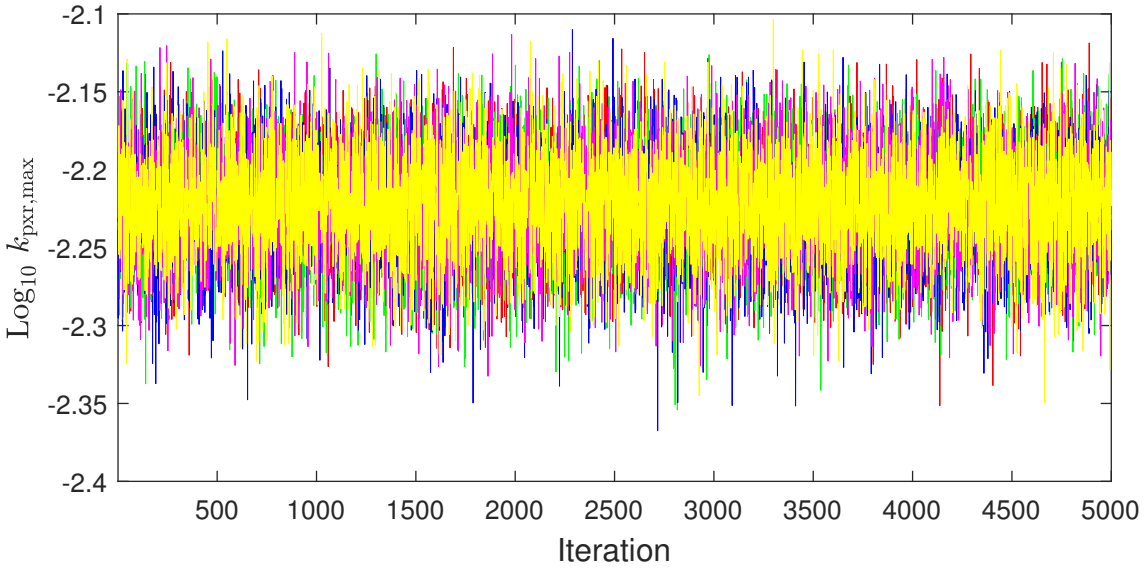

Figure S2: Trace plot for MCMC-accepted values of $k_{\mathbf{pxr,max}}$ for MC1. Equations (5)–(8) in the main text for MC1 were fitted simultaneously to the fold expression data of CYP3A4, CYP2C9, and CYP2B6 mRNA obtained from 3D PHHs treated with 25-DRIF using MCMC. Five independent chains, each depicted in a different color, were run for 50,000 steps with a burn-in period of 25,000 steps, and the chains were thinned by accepting every 5th step. We recall that in MC1, the maximum PXR activation rate constant, $k_{\mathrm{pxr,max}}$, was estimated and the PXR-dependent fold transcription rate constants $k_{mRNA^{\mathrm{fold}}_{\mathrm{cyp3a4}}}$ for CYP3A4, $k_{mRNA^{\mathrm{fold}}_{\mathrm{cyp2c9}}}$ for CYP2C9, and $k_{mRNA^{\mathrm{fold}}_{\mathrm{cyp2b6}}}$ for CYP2B6 were fixed to the values in Table 1. Details on the fitting process are in Materials and Methods in the main text.

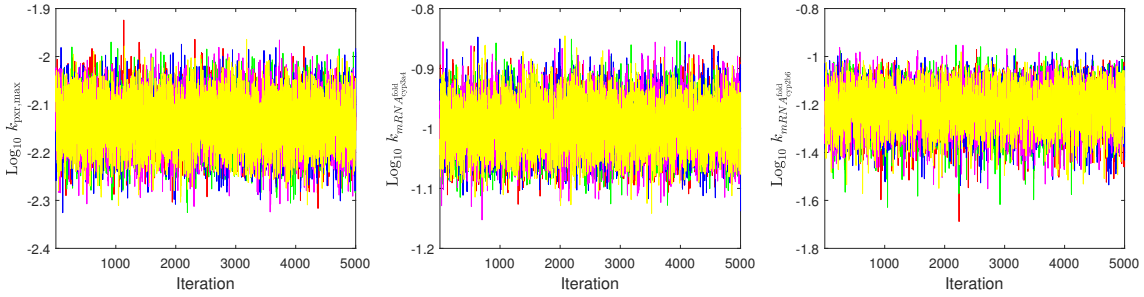

Figure S3: Trace plots for MCMC-accepted values of $k_{\mathbf{pxr,max}}$, $k_{mRNA^{\mathbf{fold}}_{\mathbf{cyp3a4}}}$, and $k_{mRNA^{\mathbf{fold}}_{\mathbf{cyp2b6}}}$ for MC2. Equations (5)–(8) in the main text for MC2 were fitted simultaneously to the fold expression data of CYP3A4, CYP2C9, and CYP2B6 mRNA obtained from 3D PHHs treated with 25-DRIF using MCMC. Five independent chains, each depicted in a different color, were run for 50,000 steps with a burn-in period of 25,000 steps, and the chains were thinned by accepting every 5th step. We recall that in MC2, the maximum PXR activation rate constant, $k_{\mathrm{pxr,max}}$, was estimated together with the PXR-dependent fold transcription rate constants $k_{mRNA^{\mathrm{fold}}_{\mathrm{cyp3a4}}}$ for CYP3A4 and $k_{mRNA^{\mathrm{fold}}_{\mathrm{cyp2b6}}}$ for CYP2B6. The PXR-dependent fold transcription rate constant $k_{mRNA^{\mathrm{fold}}_{\mathrm{cyp2c9}}}$ for CYP2C9 was assumed to be ligand independent and thus fixed to the value obtained from 3D PHHs treated with RIF (Table 1). Details on the fitting process are in Materials and Methods in the main text.

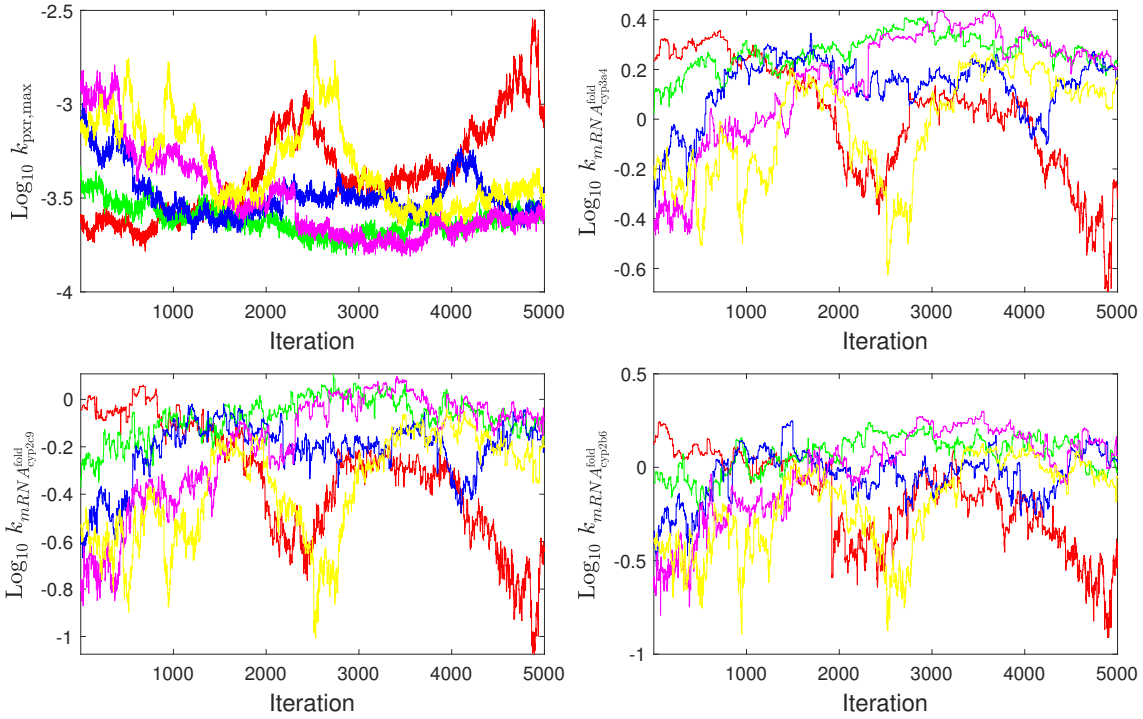

Figure S4: Trace plots for MCMC-accepted values of $k_{\mathbf{pxr,max}}$, $k_{mRNA^{\mathbf{fold}}_{\mathbf{cyp3a4}}}$, $k_{mRNA^{\mathbf{fold}}_{\mathbf{cyp2c9}}}$, and $k_{mRNA^{\mathbf{fold}}_{\mathbf{cyp2b6}}}$ for MC3. Equations (5)–(8) in the main text for MC3 were fitted simultaneously to the fold expression data of CYP3A4, CYP2C9, and CYP2B6 mRNA obtained from 3D PHHs treated with 25-DRIF using MCMC. Five independent chains, each depicted in a different color, were run for 50,000 steps with a burn-in period of 25,000 steps, and the chains were thinned by accepting every 5th step. We recall that in MC3, the maximum PXR activation rate constant, $k_{\mathrm{pxr,max}}$, was estimated together with the PXR-dependent fold transcription rate constants $k_{mRNA^{\mathrm{fold}}_{\mathrm{cyp3a4}}}$ for CYP3A4, $k_{mRNA^{\mathrm{fold}}_{\mathrm{cyp2c9}}}$ for CYP2C9, and $k_{mRNA^{\mathrm{fold}}_{\mathrm{cyp2b6}}}$ for CYP2B6. Unlike for MC1 and MC2, MCMC chains for MC3 did not converge to stationary posterior distributions. Despite MC3 being structurally identifiable for a single observed CYP mRNA fold expression profile, stringent conditions need to be fullfiled for MC3 to be structurally identifiable when all three CYP mRNA fold expression profiles are observed simultaneously and considered in the fitting (details are in Appendix A in the main text). MC3 was not practically identifiable (details are in Appendix B in the main text). Details on the fitting process are in Materials and Methods in the main text.

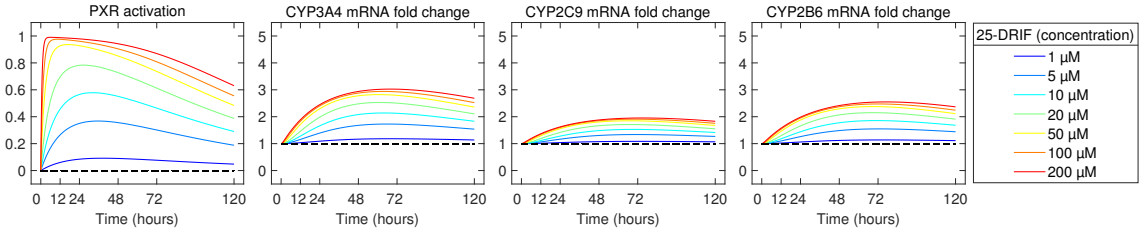

Figure S5: Predicted levels of activated PXR and fold mRNA expression of PXR-regulated genes for different 25-DRIF concentrations. Solutions of Equations (5)–(8) in the main text for MC2 for 3D PHHs treated with 25-DRIF at different concentrations were generated using best-fit parameter values in Table 1.

Sensitivity analysis

Direct sensitivity analysis

Following Dickinson and Gelinas (1976), we performed a direct sensitivity analysis for Equations (5)–(8) in the main text for MC2, with respect to the estimated parameters

$$p = \Big[k_{\text{pxr,max}}, \; k_{mRNA^{\text{fold}}_{\text{cyp3a4}}}, \; k_{mRNA^{\text{fold}}_{\text{cyp2b6}}} \Big].$$

Let y be the solution vector of Equations (5)–(8),

$$y = \Big[pxr(t), \; mRNA^{\text{fold}}_{\text{cyp3a4}}(t), \; mRNA^{\text{fold}}_{\text{cyp2c9}}(t), \; mRNA^{\text{fold}}_{\text{cyp2b6}}(t) \Big],$$

and

$$\frac{\partial y}{\partial t} = f(t, y; p)$$

its derivative, where $f(t, y; p)$ is a collection of the right-hand sides of Equations (5)–(8). The sensitivity functions, $S_i(t)$, are defined as the derivatives of the solutions of Equations (5)–(8) with respect to the estimated parameter, c, in the parameter vector p,

$$S_i(t) = \frac{\partial y_i}{\partial c}, \qquad 1 \leq i \leq n, \tag{S.1}$$

where n is the number of equations in the system (5)–(8), that is, $n = 4$.

By applying the chain rule for differentiation and the rule for interchanging the order of differentiation for mixed second partials, one obtains the sensitivity equations

$$\frac{dS}{dt} = J(t, y; p)\, S + \frac{\partial f(t, y; p)}{\partial c} \tag{S.2}$$

$$S_i(t_0) = \frac{\partial y_0}{\partial c} = 0, \qquad 1 \leq i \leq n, \tag{S.3}$$

where $S = [S_1, \ldots, S_n]$, and $J(t, y; p)$ is the Jacobian of Equations (5)–(8) given as

$$J(t,y;p) = \begin{bmatrix} -\left(k_{\text{pxr,max}}\, C_{25-\text{drif}}\, e^{-k_\text{r}\, t} + k_{\text{pxr,deg}}\right) & 0 & 0 & 0 \\ k_{mRNA^{\text{fold}}_{\text{cyp3a4}}} & -k_{mRNA_{\text{cyp3a4,deg}}} & 0 & 0 \\ k_{mRNA^{\text{fold}}_{\text{cyp2c9}}} & 0 & -k_{mRNA_{\text{cyp2c9,deg}}} & 0 \\ k_{mRNA^{\text{fold}}_{\text{cyp2b6}}} & 0 & 0 & -k_{mRNA_{\text{cyp2b6,deg}}} \end{bmatrix}. \tag{S.4}$$

Since the initial conditions of Equations (5)–(8) do not depend on any parameter from the vector p, the initial conditions for all sensitivities are zero, that is, $S_i(t_0) = 0$ for $\forall i = 1, \ldots, n$ (Equation (S.3)).

The matrix of all partial derivatives of $f(t, y; p)$ with respect to the parameter vector p is as follows:

$$\left[\frac{\partial f(t,y;p)}{\partial p}\right] = \begin{bmatrix} (1-[pxr])\, C_{25-\text{drif}}\, e^{-k_\text{r}\, t} & 0 & 0 \\ 0 & [pxr] & 0 \\ 0 & 0 & 0 \\ 0 & 0 & [pxr] \end{bmatrix}. \tag{S.5}$$

The sensitivity system for a parameter c is thus in the form

$$\frac{dS}{dt} = \begin{bmatrix} -\left(k_{\text{pxr,max}}\, C_{25-\text{drif}}\, e^{-k_\text{r}\, t} + k_{\text{pxr,deg}}\right)\, S_1 \\ k_{mRNA^{\text{fold}}_{\text{cyp3a4}}}\, S_1 - k_{mRNA_{\text{cyp3a4,deg}}}\, S_2 \\ k_{mRNA^{\text{fold}}_{\text{cyp2c9}}}\, S_1 - k_{mRNA_{\text{cyp2c9,deg}}}\, S_3 \\ k_{mRNA^{\text{fold}}_{\text{cyp2b6}}}\, S_1 - k_{mRNA_{\text{cyp2b6,deg}}}\, S_4 \end{bmatrix} + \begin{bmatrix} \frac{\partial f_1}{\partial c} \\ \frac{\partial f_2}{\partial c} \\ \frac{\partial f_3}{\partial c} \\ \frac{\partial f_4}{\partial c} \end{bmatrix}. \tag{S.6}$$

Finally, we solve Equations (5)–(8) simultaneously with Equations (S.6). Since the individual parameters in the parameter vector p of the system (5)–(8), c, are treated independently, we can solve the sensitivities for one parameter at a time.

In our analysis, we consider the normalized sensitivity coefficients expressed as

$$s_i(c) = \frac{\partial \log(y_i(t,p))}{\partial \log(c)} = \frac{\partial y_i(t,p)}{\partial c}\frac{c}{y_i(t,p)} = c\,\frac{S_i(t)}{y_i(t,p)}, \tag{S.7}$$

which are dimensionless and allow to track the relative change in the solutions that is observed when a positive perturbation to the parameter is applied.

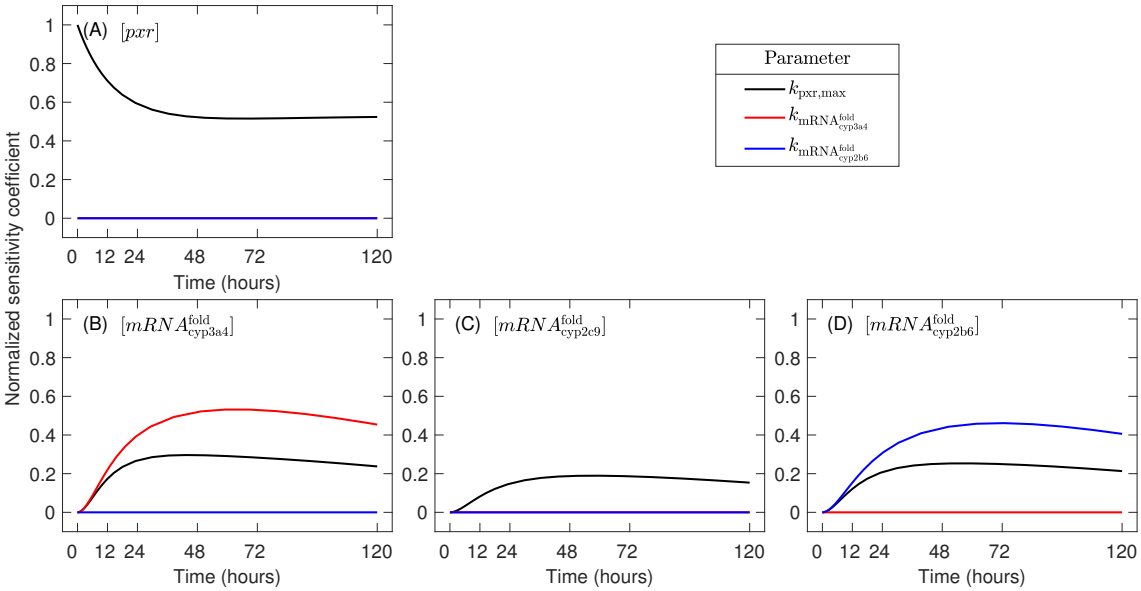

Figure S6: Direct sensitivity analysis. Sensitivities were expressed as normalized sensitivity coefficients for MC2. The following parameters were considered: $k_{\text{pxr,max}}$, $k_{mRNA^{\text{fold}}_{\text{cyp3a4}}}$, and $k_{mRNA^{\text{fold}}_{\text{cyp2b6}}}$. The following variables were considered: (A) $[pxr]$, (B) $[mRNA^{\text{fold}}_{\text{cyp3a4}}]$, (C) $[mRNA^{\text{fold}}_{\text{cyp2c9}}]$, and (D) $[mRNA^{\text{fold}}_{\text{cyp2b6}}]$. Parameters to which the variables were insensitive produced zero normalized sensitivity coefficients and consequently appeared as flat lines. The parameter values were fixed at their best-fit values (Table 1 in the main text).

Local sensitivity analysis

To assess how varying the model parameters, $k_{\text{pxr,max}}$, $k_{mRNA^{\text{fold}}_{\text{cyp3a4}}}$, and $k_{mRNA^{\text{fold}}_{\text{cyp2b6}}}$, influences the solutions of Equations (5)–(8) in the main text, a one-at-a-time (OAT) sensitivity analysis was performed. Each parameter was varied independently by $\pm 50\%$ from its maximum likelihood estimate (best-fit) while holding all other parameters constant. The model configuration considered was MC2.

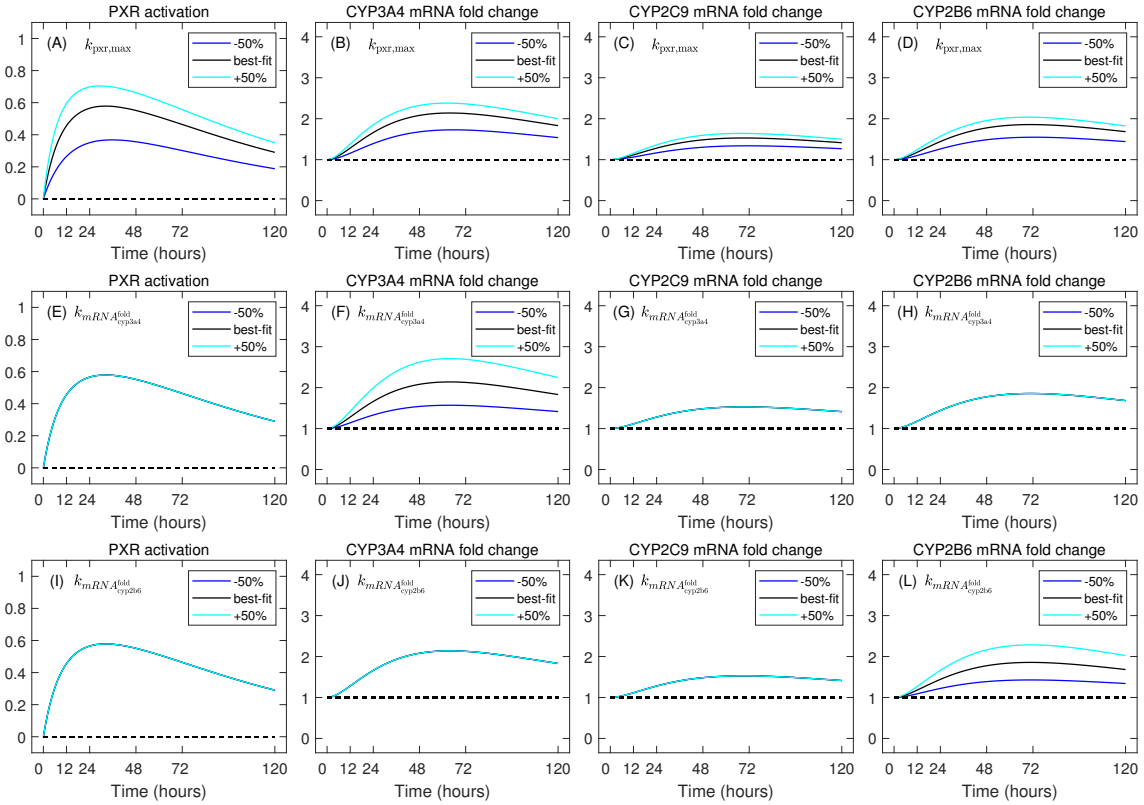

Figure S7: OAT sensitivity analysis. The parameters $k_{\mathrm{pxr,max}}$, $k_{mRNA^{\mathrm{fold}}_{\mathrm{cyp3a4}}}$, and $k_{mRNA^{\mathrm{fold}}_{\mathrm{cyp2b6}}}$ were varied by 50% from the best-fit values (Table 1 in the main text) and the corresponding solutions of MC2 were displayed as follows: A black solid line was used for the solutions associated with the best-fit parameter values; a cyan solid line was used for the solutions associated with perturbations in the best-fit parameter values by +50%; a blue solid line was used for the solutions associated with perturbations in the best-fit parameter values by −50%.

References

Dickinson RP, Gelinas RJ (1976) Sensitivity analysis of ordinary differential equation systems – a direct method. Journal of Computational Physics 21(2):123–143